

cells. Focusing on *NRAS*, known as an oncogene, we analyzed it, and identified a CAA→AAA substitution at codon 61, resulting in a Glu→Lys change at position 61. When the mutant *NRAS* was transfected into fibroblasts for its expression, many transformed foci were generated, confirming the transforming ability of the mutant *NRAS*.

The RAS gene family is a group of three oncogenes, *KRAS*, *HRAS*, and *NRAS*, which are most commonly activated in human malignant neoplasms (16). For RAS activation, an amino acid substitution at position 12, 13, 59, or 61 is important. It was reported in thyroid tumors that a CAA→CGA substitution at codon 61 of *NRAS* resulted in a Glu→Arg change at position 61 and *NRAS* activation (17). It was also noted in the neuroblastoma cell line SK-N-SH that a Glu→Lys mutation at position 61 of *NRAS* resulted in its activation (18).

Furthermore, *KRAS* mutations were reported to occur in about 50% of ovarian mucinous carcinomas (19,20) and 30% of serous borderline ovarian tumors (21). In addition, *HRAS* mutations were reported in about 6% of ovarian cancers (22). However, no *NRAS* activation in ovarian cancers has been reported to date (22). Since the cell proliferation function of the *HRAS*, *KRAS*, and *NRAS* gene products overlaps with one another in many cases, the reason for selective *KRAS* activation in specific histological types of ovarian cancer is unclear.

This study is the first in the world to identify *NRAS* gene activation by point mutation in an ovarian cancer cell line. However, no *NRAS* gene activation has been reported in ovarian cancer patients. In the future, it will be necessary to analyze clinical samples for *NRAS* mutations, particularly amino acid substitutions at position 61. TYK-CPr, in which an activated *NRAS* gene was identified in this study, is a cell line derived from an undifferentiated ovarian cancer with a clinically poor prognosis. This suggests that *NRAS* activation is associated with specific histological types of ovarian cancer.

Recently, sorafenib, a molecular-targeted therapeutic drug targeting activated RAS, has been developed and used clinically. The drug inhibits Raf kinase downstream of RAS, thereby blocking the RAS/MEK/ERK signaling pathway and exerting antitumor effects (23). Such a molecular-targeted drug may be effective for ovarian cancer patients with the *NRAS* mutations reported here.

Among the genes screened in this study, proteasome has been reported to be involved in cell cycle regulation and apoptosis (24). In addition, *keratin 8* has been reported to be involved in malignant transformation and cancer cell invasion (25). These genes may be ovarian cancer-related oncogenes, although further studies are needed.

## References

- Jemal A, Siegel R and Ward E: Cancer statistics, 2008. *CA Cancer J Clin* 58: 71-76, 2008.
- Armstrong DK, Bundy B and Wenzel L: Intraperitoneal cisplatin and paclitaxel in ovarian cancer. *N Engl J Med* 354: 34-43, 2006.
- Druker BJ, Talpaz M and Resta DJ: Efficacy and safety of a specific inhibitor of the BCR-ABL tyrosine kinase in chronic myeloid leukemia. *N Engl J Med* 344: 1031-1037, 2001.
- Maloney DG, Grillo-Lopez AJ and White CA: IDEC-C2B8 (Rituximab) anti-CD20 monoclonal antibody therapy in patients with relapsed low-grade non-Hodgkin's lymphoma. *Blood* 90: 2188-2195, 1997.
- Okamoto A, Sameshima Y and Yokoyama S: Frequent allelic losses and mutations of the p53 gene in human ovarian cancer. *Cancer Res* 51: 5171-5176, 1991.
- Esteller M, Silva JM and Dominguez G: Promoter hypermethylation and BRCA1 inactivation in sporadic breast and ovarian tumors. *J Natl Cancer Inst* 92: 564-569, 2000.
- Soda M, Choi YL and Enomoto M: Identification of the transforming EML4-ALK fusion gene in non-small-cell lung cancer. *Nature* 448: 545-546, 2007.
- Imai S, Kiyozuka Y and Maeda H: Establishment and characterization of a human ovarian serous cystadenocarcinoma cell line that produces the tumor markers CA-125 and tissue polypeptide antigen. *Oncology* 47: 177-184, 1990.
- Yoshizawa H, Adashi S and Misawa Y: Isolation of cisplatin-resistant subline from human ovarian cancer cell line and analysis of its cell-biological characteristics (in Japanese). *Nihon Sanfujinka Gakkai-shi* 141: 7-14, 1989.
- Pear WS, Nolan GP and Scott ML: Production of high-titer helper-free retroviruses by transient transfection. *Proc Natl Acad Sci USA* 90: 8392-8396, 1993.
- Onishi M, Kinoshita S and Morikawa Y: Applications of retrovirus-mediated expression cloning. *Exp Hematol* 24: 324-329, 1996.
- Kent WJ: BLAT - the BLAST-like alignment tool. *Genome Res* 12: 656-664, 2002.
- Aaronson SA: Growth factors and cancer. *Science* 254: 1146-1153, 1991.
- Kisanuki H, Choi YL and Wada T: Retroviral expression screening of oncogenes in pancreatic ductal carcinoma. *Eur J Cancer* 41: 2170-2175, 2005.
- Choi YL, Moriuchi R and Osawa M: Retroviral expression screening of oncogenes in natural killer cell leukemia. *Leuk Res* 29: 943-949, 2005.
- Shih TY and Weeks MO: Oncogenes and cancer: the p21 ras genes. *Cancer Invest* 2: 109-123, 1984.
- Nikiforova MN, Lynch RA and Biddinger PW: RAS point mutations and PAX8-PPAR gamma rearrangement in thyroid tumors: evidence for distinct molecular pathways in thyroid follicular carcinoma. *J Clin Endocrinol Metab* 88: 2318-2326, 2003.
- Taparowsky E, Shimizu K and Goldfarb M: Structure and activation of the human N-ras gene. *Cell* 34: 581-586, 1983.
- Ichikawa Y, Nishida M and Suzuki H: Suppression of metastasis of rat prostatic cancer by introducing human chromosome 8. *Cancer Res* 54: 2299-2302, 1994.
- Suzuki M, Saito S and Saga Y: Mutation of K-RAS proto-oncogene and loss of heterozygosity on 6q27 in serous and mucinous ovarian carcinomas. *Cancer Genet Cytogenet* 118: 132-135, 2000.
- Shih IeM and Kurman RJ: Molecular pathogenesis of ovarian borderline tumors: new insights and old challenges. *Clin Cancer Res* 11: 7273-7279, 2005.
- Mammas IN, Zafiropoulos A and Spandidos DA: Involvement of the ras genes in female genital tract cancer (review). *Int J Oncol* 26: 1241-1255, 2005.
- Zhang X, Vincent P and McHugh M: BAY 43-9006 exhibits broad spectrum oral antitumor activity and targets the RAF/MEK/ERK pathway and receptor tyrosine kinases involved in tumor progression and angiogenesis. *Cancer Res* 64: 7099-7109, 2004.
- Wilhelm SM, Carter C and Tang L: Proteasome inhibition and its clinical prospects in the treatment of hematologic and solid malignancies. *Cancer* 104: 1794-1807, 2005.
- Hendrix MJC, Seftor EA and Chu YW: Role of intermediate filaments in migration, invasion and metastasis. *Cancer Metastasis Rev* 15: 507-525, 1996.

## Schedule-dependent synergism and antagonism between pemetrexed and docetaxel in human lung cancer cell lines in vitro

Yasuhiko Kano · Masaru Tanaka · Miyuki Akutsu · Kiyoshi Mori · Yasuo Yazawa · Hiroyuki Mano · Yusuke Furukawa

Received: 26 August 2008 / Accepted: 27 February 2009 / Published online: 22 March 2009  
© Springer-Verlag 2009

### Abstract

**Background** Pemetrexed and docetaxel show clinical activities against a variety of solid tumors including lung cancers. To identify the optimal schedule for combination, cytotoxic interactions between pemetrexed and docetaxel were studied at various schedules using three human lung cancer cell lines A-549, Lu-99, and SBC-5 in vitro.

**Methods** Cells were incubated with pemetrexed and docetaxel simultaneously for 24 or 120 h. Cells were also incubated with pemetrexed for 24 h, followed by a 24 h exposure to docetaxel, and vice versa. Growth inhibition was determined using 3-(4,5-dimethylthiazol-2-yl)-2,5-diphenyltetrazolium bromide (MTT) assay and cell cycle

analysis. Cytotoxic interactions were evaluated by the isobologram method.

**Results** Simultaneous exposure to pemetrexed and docetaxel for 24 and 120 h produced antagonistic effects in all three cell lines. Pemetrexed (24 h) followed by docetaxel (24 h) produced additive effects in A-549 cells and synergistic effects in Lu-99 and SBC-5 cells. Docetaxel followed by pemetrexed produced additive effects in A-549 and Lu-99 cells and antagonistic effects in SBC-5 cells. The results of cell cycle analysis were fully consistent with those of isobologram analysis, and provide the molecular basis of the sequence-dependent difference in cytotoxic interactions between the two agents.

**Conclusions** Sequential administration of pemetrexed followed by docetaxel may provide the greatest anti-tumor effects for this combination in the treatment of lung cancer.

Y. Kano (✉) · M. Tanaka · M. Akutsu  
Division of Hematology,  
Tochigi Cancer Center, Yonan,  
Utsunomiya, Tochigi 320-0834, Japan  
e-mail: ykano@tcc.pref.tochigi.jp

K. Mori  
Division of Thoracic Diseases,  
Tochigi Cancer Center, Utsunomiya,  
Tochigi 320-0834, Japan

Y. Yazawa  
Division of Orthopedic Oncology,  
Tochigi Cancer Center, Utsunomiya,  
Tochigi 320-0834, Japan

H. Mano  
Division of Functional Genomics,  
Jichi Medical University,  
Tochigi 329-0431, Japan

Y. Furukawa  
Division of Stem Cell Regulation,  
Jichi Medical University,  
Tochigi 329-0431, Japan

**Keywords** Pemetrexed · Docetaxel · Isobologram · Lung cancer

### Introduction

Lung cancer is the leading cause of cancer mortality in industrialized countries, with non-small cell lung cancer (NSCLC) accounting for nearly 80% [1]. Although surgery may be curative in early-stage NSCLC, most patients present with inoperable advanced disease. These patients managed with best supportive care alone have a median survival time of only 5 months and a 1-year survival rate of approximately 10% [2]. First-line treatment for patients with advanced NSCLC includes platinum compounds combined with vinorelbine, gemcitabine, or taxanes [3]. This is associated with improved quality of life, but only moderate survival advantages when compared with best supportive

care alone. Therefore, there is an emergent need for effective second-line treatments for NSCLC patients who experience disease progression after first-line chemotherapy. Currently, erlotinib, docetaxel, and pemetrexed are approved as second-line drugs by the US Food and Drug Administration for patients whose tumors have progressed after platinum-based treatments [4, 5].

Small cell lung cancer (SCLC) accounts for approximately 12% of all lung cancers [6]. Compared with NSCLC, SCLC has a rapid doubling time, and earlier development of wide spread metastasis. SCLC is highly sensitive to initial radiotherapy and chemotherapy. The most commonly used regimens include etoposide, cisplatin, doxorubicin, or cyclophosphamide [7]. For limited-stage patients, chemotherapy associated with thoracic radiation was able to produce a cure rate of 10–20%. In extensive disease, the combinations of these agents yields responses of 50–70%, with 20–30% complete remissions, but most patients die from recurrent diseases. The identification of new agents is critical for further progress in the treatment of SCLC, and the evaluation of a variety of agents including docetaxel and pemetrexed has been underway [8–10].

Pemetrexed is a new antifolate that has significant activity against a broad spectrum of solid tumors including lung cancer [11, 12]. Pemetrexed inhibits multiple enzymes involved in folate metabolism including thymidylate synthase, dihydrofolate reductase, and glycinamide ribonucleotide formyltransferase [13]. Pemetrexed arrests cells mainly in S phase and induces apoptosis against tumor cells [14]. Against lung cancers, pemetrexed is non-inferior to docetaxel, with lower hematologic toxicity, and febrile neutropenia and a similar rate of non-hematologic toxicities [12].

The taxanes, paclitaxel and docetaxel, have significant activity in lung cancer. Both inhibit microtubule dynamics and cause G2/M cell cycle arrest. However, there are several differences between them in the pharmacokinetics and pharmacologic actions [15, 16]. Docetaxel demonstrated greater affinity for the tubulin-binding site, wider cell cycle activity, longer intracellular retention time and higher intracellular concentration in tumor cells, more potent antitumor activity in *in vitro* and *in vivo* models, and more potent induction of bcl-2 phosphorylation and apoptosis. Paclitaxel has a non-linear pharmacokinetic behavior, while docetaxel demonstrated linear pharmacokinetics and less schedule dependence than paclitaxel.

The combination of pemetrexed and docetaxel may play a major role in the second-line treatment of lung cancers. The wide range of antitumor activity of these agents, their different cytotoxic mechanisms and different toxicity profiles, and the absence of cross-resistance provide the rationale for combining these agents. Since both pemetrexed and docetaxel are cell cycle-specific, disturbances of the cell cycle produced by one drug may influence the cytotoxic

effects of the other. Furthermore the drug schedule may play a significant role in the outcome, and therefore, how the drugs are combined requires careful consideration.

We showed that the ordered treatment of pemetrexed followed by paclitaxel may be synergistic, whereas simultaneous administration was potentially antagonistic in a variety of solid tumor cell lines [17]. What is not clear is whether such schedule dependency will be as important for pemetrexed and docetaxel as for pemetrexed and paclitaxel in the treatment of lung cancers. The present study was aimed at characterizing the cytotoxic effects of various pemetrexed and docetaxel combinations and schedules on three human lung cancer cell lines using the isobologram method of Steel and Peckham [18]. Flow cytometry was performed to understand the molecular basis of the schedule-dependent synergism and antagonism of the pemetrexed and docetaxel combination.

## Materials and methods

### Cell lines

Three human lung cancer lines, A-549 (lung adenocarcinoma), Lu-99 (giant-cell lung cancer), and SBC-5 (small cell lung cancer) were used. A-549 cells were purchased from the American Type Culture Collection (Rockville, MD). Lu-99 and SBC-5 cells were obtained from Health Science Research Resources Bank (Tokyo). These cells were growing as a monolayer in 75-cm<sup>2</sup> plastic tissue culture flasks containing RPMI1640 medium (Sigma Chemical Co., St Louis, MO) supplemented with 10% heat-inactivated fetal bovine serum (FBS) (Sigma) and antibiotics (penicillin G and streptomycin) in a humidified atmosphere of 95% air/5% CO<sub>2</sub> at 37°C. Under these conditions, the doubling times of these cells were 20–30 h.

### Drugs

Pemetrexed and docetaxel were kindly provided by Eli Lilly and Company (Indianapolis, IN) and Sanofi-Aventis K.K. (Tokyo, Japan), respectively. Drugs were dissolved with RPMI1640 and stored at –80°C. Drugs were diluted with RPMI-1640 plus 10% FBS before use.

### Cell growth inhibition using combined anti-cancer agents

Growing cells were collected by trypsinization, separated and resuspended to a final concentration of  $5.0 \times 10^3$  cells/ml in fresh medium containing 10% FBS and antibiotics. Cell suspensions (100  $\mu$ l) were dispensed into the individual wells of a 96-well tissue culture plate with a lid (Costar, Corning, NY). Each plate had one 8-well control column

containing medium alone and one 8-well control column containing cells but no drug. Eight plates were prepared for each drug combination.

#### Simultaneous and continuous exposure to pemetrexed and docetaxel

After a 20–24 h incubation for cell attachment, solutions of docetaxel and pemetrexed (50  $\mu$ l) at different concentrations were added to individual wells in final volumes of 200  $\mu$ l per wells. The plates were incubated under the same conditions for 120 h.

#### Simultaneous 24 h exposure to pemetrexed and docetaxel

After cell attachment, solutions of docetaxel and pemetrexed (50  $\mu$ l) at different concentrations were added to individual wells in final volumes of 200  $\mu$ l per wells. The plates were also incubated under the same conditions for 24 h. The cells were then washed twice with culture medium, and then fresh medium (200  $\mu$ l) and antibiotics were added. The cells were cultured again for four additional days in drug-free medium.

#### Sequential exposure to pemetrexed (24 h) followed by docetaxel (24 h) or vice versa

After cell attachment, medium containing 10% FBS (50  $\mu$ l) and solutions of docetaxel or pemetrexed (50  $\mu$ l) at different concentrations were added to individual wells. The plates were then incubated under the same conditions for 24 h. The cells were washed twice and fresh medium was added, followed by the addition of solutions of docetaxel or pemetrexed (50  $\mu$ l) at different concentrations. The plates were incubated again under the same conditions for 24 h. The cells were then washed twice, and the cells were cultured for three additional days in drug-free medium.

#### MTT assay

Viable cell growth was determined by 3-(4,5-dimethylthiazol-2-yl)-2,5-diphenyltetrazolium bromide (MTT) assay [19]. For all 4 cell lines examined, we established a linear relation between the MTT assay value and the cell number within the range shown.

#### Isobologram

The dose–response interactions between pemetrexed and docetaxel were evaluated at the  $IC_{50}$  level by the isobologram method of Steel and Peckham (Fig. 1) [18]. The  $IC_{50}$  was defined as the concentration of drug that produced 50% cell growth inhibition; i.e. a 50% reduction of absorbance.

The theoretical basis of the isobologram method and the procedure for making the isobologram has been described in detail [18, 20, 21]. Based on the dose–response curves of pemetrexed and docetaxel, three isoeffect curves were constructed (Fig. 1). If the agents act additively by independent mechanisms, combined data points would lie near the Mode I line (hetero-addition). If the agents act additively by similar mechanisms, the combined data points would lie near the Mode II lines (iso-addition) [14, 16, 17].

Since we cannot know in advance whether the combined effects of two agents will be hetero-additive, iso-additive, or an effective intermediate between these extremes, all possibilities should be considered. Thus, when the data points of the drug combination fell within the area surrounded by mode I and/or mode II lines (i.e. within the envelope of additivity), the combination was described as additive.

We used this envelope to evaluate not only the simultaneous exposure combinations of pemetrexed and docetaxel, but also to evaluate the sequential exposure combinations, since the second agent under our experimental conditions could modulate the cytotoxicity of the first agent.

A combination that gives data points to the left of the envelope of additivity (i.e. the combined effect is caused by lower doses of the two agents than is predicted) can confidently be described as supra-additive (synergism). A combination that gives data points to the right of the

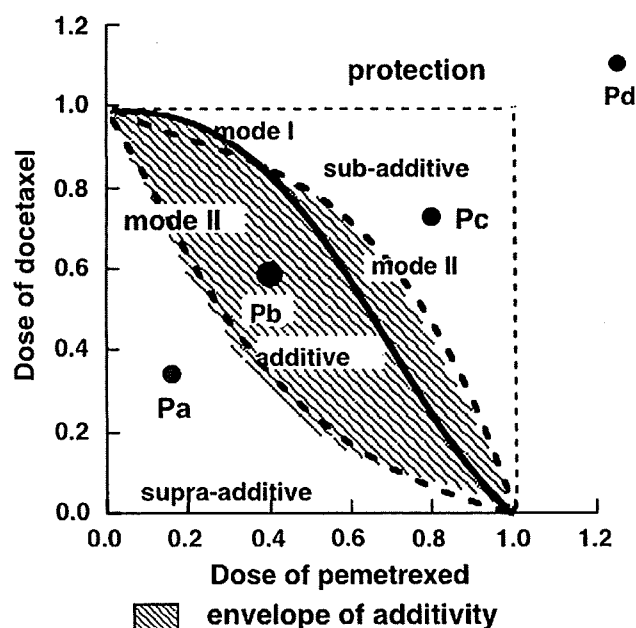


**Fig. 1** Schematic representation of an isobologram (Steel and Peckham). The envelope of additivity, surrounded by mode I (solid line) and mode II (dotted lines) isobologram lines, was constructed from the dose–response curves of pemetrexed alone and docetaxel alone. The concentrations that produced 50% cell growth inhibition were expressed as 1.0 in the ordinate and the abscissa. Combined data points *Pa*, *Pb*, *Pc* and *Pd* show supra-additive, additive, sub-additive, and protective effects, respectively

envelope of additivity, but within the square or on the line of the square can be described as sub-additive (i.e. the combination is superior or equal to a single agent but is less than additive). A combination that gives data points outside the square can be described as protective (i.e. the combination is inferior in cytotoxic action to a single agent). A combination with both sub-additive and/or protective interactions can confidently be described as antagonistic.

#### Data analysis

Findings were analyzed as described previously [22]. To determine whether the condition of synergism (or antagonism) truly existed, a Wilcoxon signed-rank test was performed to compare the observed data with the predicted minimum (or maximum) data for an additive effect. Probability values ( $P \leq 0.05$ ) were considered significant. Combinations with  $P > 0.05$  were regarded as having an additive/synergistic (or additive/antagonistic) effect. All statistical analyses were performed using the Stat View 4.01 software program (Abacus Concepts, Berkeley, CA).

#### Flow cytometric analysis

SBC-5 cells were treated with 5.0  $\mu\text{M}$  pemetrexed alone, or 1.5 nM docetaxel alone or their combination simultaneously for 24 h. The cells were also treated with pemetrexed for 24 h followed by docetaxel for 24 h or the reverse sequence. The cells were harvested at 72 h and the cell cycle profiles were analyzed by staining intracellular DNA with propidium iodide in preparation for flow cytometry with the FACScan · CellFIT system (Becton-Dickinson, San Jose, CA). The size of the sub-G1, G0/G1 and S+G2/M fractions was calculated as a percentage by analyzing DNA histograms with the ModFitLT 2.0 program (Verity Software, Topsham, ME) [23].

#### Results

Figure 2 shows the dose–response curves for pemetrexed in A-549, Lu-99, and SBC-5 cells. The dose–response curves were plotted on a semi-log scale as a percentage of the control. The  $\text{IC}_{50}$  values of pemetrexed against these cells were  $1.5 \pm 0.4$ ,  $0.42 \pm 0.10$ ,  $1.3 \pm 0.2$   $\mu\text{M}$ , respectively ( $n = 5$ ). The  $\text{IC}_{50}$  values of docetaxel against these cells were  $1.7 \pm 0.2$ ,  $1.0 \pm 0.1$ , and  $0.82 \pm 0.13$  nM, respectively ( $n = 5$ ).

The dose–response curves in Fig. 3 show the effect of simultaneous exposure (24 h) (panel a), sequential exposure to pemetrexed followed by docetaxel (panel b), and vice versa (panel c) on the growth of SBC-5 cells. The

#### Dose–response curves of pemetrexed against lung cancer cell lines

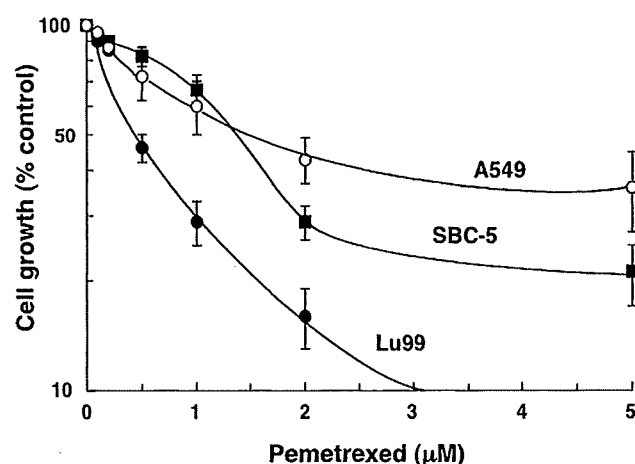


**Fig. 2** The dose–response curves of 24 h exposure to pemetrexed against A-549, Lu-99, and SBC-5 cells. Cell growth inhibition was measured using the MTT assay after 5 days and was plotted as a percentage of the control (cells not exposed to drugs). Each point represents the mean  $\pm$  SEM for at least three independent experiments

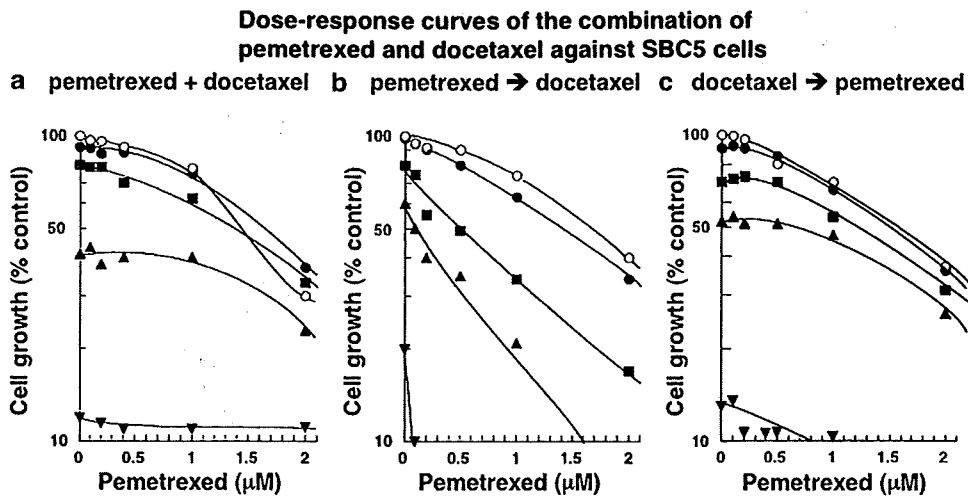
pemetrexed concentrations are shown on the abscissa. Dose–response curves in which the docetaxel concentrations are shown on the abscissa are based on the same data (figure not shown). Three isoeffect curves (mode I and mode II lines) were constructed based on the dose–response curves of pemetrexed alone and docetaxel alone. Isobolograms at the  $\text{IC}_{50}$  level were generated based on these dose–response curves for the combinations.

#### Simultaneous exposure to docetaxel and pemetrexed for 24 h

Figure 4a shows isobolograms of SBC-5 cells after simultaneous exposure to pemetrexed and docetaxel. The combined data points fell in the areas of subadditivity and protection. The mean values of the observed data (0.71) were larger than those of the predicted maximum values (0.60). The observed data and the predicted maximum data were compared by Wilcoxon signed-rank test. The difference was significant ( $P < 0.05$ ), indicating antagonistic effects (Table 1). Quite similar effects were observed in A-549 and Lu-99 cells (Table 1, isobolograms not shown).

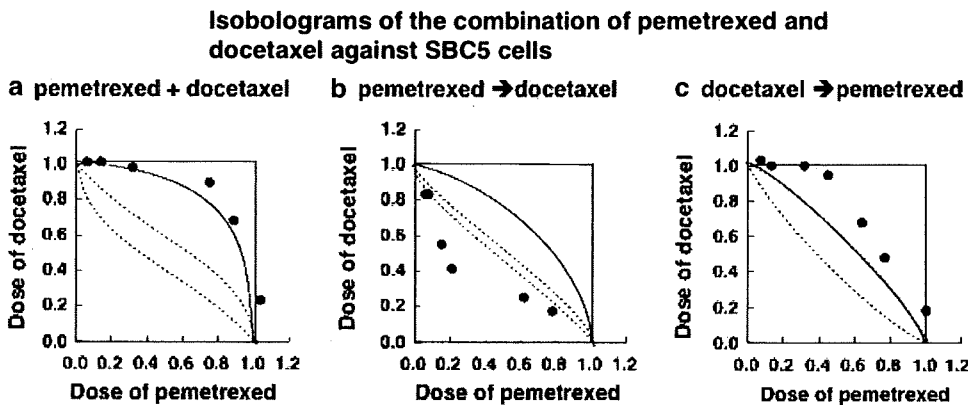
#### Sequential exposure to pemetrexed for 24 h followed by docetaxel for 24 h

Figure 4b shows isobolograms of SBC-5 cells exposed first to pemetrexed and then to docetaxel. The combined data points fell in the area of supraadditivity. The mean values of the observed data (0.46) were smaller than those



**Fig. 3** Schedule dependence of the interaction between docetaxel and pemetrexed in SBC-5 cells. Cells were exposed to these two drugs simultaneously for 24 h (a), pemetrexed first for 24 h followed by docetaxel for 24 h (b), and vice versa (c). The cell number after 5 days was measured using the MTT assay and was plotted as a percentage of

the control (cells not exposed to drugs). The concentrations of docetaxel are shown on the abscissa. The concentrations of pemetrexed were 0 (open circle), 0.2 (filled circle), 0.5 (filled square), 1.0 (filled triangle) and 2.0 (filled inverted triangle) µM, respectively. Data are mean values for three independent experiments; SE was < 25%



**Fig. 4** Isobolograms of simultaneous exposure to docetaxel and pemetrexed for 24 h in SBC-5 cells (a). The combined data points fell in the areas of subadditivity and protection. Data are mean values for at least three independent experiments; SE was <25%. Isobolograms of sequential exposure to pemetrexed (24 h) followed by docetaxel (24 h) in SBC-5 cells (b). All data points of the combinations fell in the area

of supraadditivity. Data are mean values for at least three independent experiments; SE was <20%. Isobolograms of sequential exposure to docetaxel (24 h) followed by pemetrexed (24 h) in SBC-5 cells (c). All data points of the combinations fell in the areas of subadditivity and protection. Data are mean values for at least three independent experiments; SE was <25%

of the predicted minimum values (0.60) (Table 1). The difference was significant ( $P < 0.05$ ), indicating synergistic effects. Quite similar effects were observed in Lu-99 cells (Table 1, isobolograms not shown), while additive effects were observed in A-549 cells (Table 1, isobolograms not shown).

**Sequential exposure to docetaxel for 24 h followed by pemetrexed for 24 h**

Figure 4c shows isobolograms of SBC-5 cells exposed first to docetaxel, followed by pemetrexed. The combined data points mainly fell in the area of subadditivity. The mean values of the observed data were larger than those of the

predicted maximum values ( $P < 0.02$ ) (Table 1), indicating antagonistic effects. For A-549 and Lu-99 cells, most combined data points fell within the envelope of additivity and the mean values of the observed data were between those of the predicted minimum and maximum values (Table 1, isobolograms not shown), indicating an additive effect of this schedule.

**Simultaneous exposure to pemetrexed and docetaxel for 5 days**

For all three cell lines, combined data points fell in the areas of subadditivity and protection, indicating antagonistic effects (Table 1, isobolograms not shown).

**Table 1** Mean values of observed data, predicted minimum, and predicted maximum of pemetrexed and docetaxel in combination at IC<sub>50</sub> level

Schedule	Cell line	n <sup>a</sup>	Observed data	Predicted min. <sup>b</sup>	Predicted max. <sup>c</sup>	Effects
Pemetrexed + docetaxel (24 h)	A-549	8	0.72	0.31	0.55	Antagonism ( $P < 0.02$ )
	Lu-99	6	>1.0	0.41	0.62	Antagonism ( $P < 0.05$ )
	SBC-5	6	0.71	0.33	0.60	Antagonism ( $P < 0.05$ )
Pemetrexed (24 h) → docetaxel (24 h)	A-549	7	0.63	0.31	0.92	Additive
	Lu-99	7	0.29	0.50	0.67	Synergism ( $P < 0.02$ )
	SBC-5	7	0.46	0.60	0.82	Synergism ( $P < 0.02$ )
Docetaxel (24 h) → pemetrexed (24 h)	A-549	8	0.64	0.32	0.86	Additive
	Lu-99	8	0.63	0.32	0.85	Additive
	SBC-5	7	0.87	0.36	0.70	Antagonism ( $P < 0.02$ )
Pemetrexed + docetaxel (5 day)	A-549	6	0.79	0.51	0.68	Antagonism ( $P < 0.05$ )
	Lu-99	6	0.96	0.45	0.62	Antagonism ( $P < 0.05$ )
	SBC-5	4	0.73	0.20	0.57	Antagonism ( $P < 0.05$ )

<sup>a</sup> Number of data points<sup>b</sup> Predicted minimum value for an additive effect<sup>c</sup> Predicted maximum value for an additive effect

### Cell cycle analysis

The isobologram analysis revealed that pemetrexed and docetaxel had a synergistic effect on two of the three lung cancer cell lines when sequentially administered with pemetrexed first and followed by docetaxel. In contrast, either simultaneous exposure or sequential addition in the reversed order (docetaxel to pemetrexed) resulted in antagonistic or additive effects. We confirmed these results by calculating the size of sub-G1 fractions, which correspond to apoptotic populations, on flow cytometry. As shown in Fig. 5, apoptosis-inducing effects of the two drugs were strongest when cells were exposed to pemetrexed first and followed by docetaxel. In contrast, the cytotoxic effects of

docetaxel were significantly suppressed when pemetrexed was added simultaneously or afterward. These data are fully consistent with the results of isobologram analysis.

Cell cycle analysis also provided a clue to understand the mechanisms underlying this observation. Pemetrexed alone induced cell cycle arrest in late G1 to early S phase in SBC-5 cells (see Fig. 6 for representative results, and Table 2 for quantification and statistical analysis of three independent experiments). Docetaxel alone caused the loss of mitotic fractions along with massive apoptosis at a relatively low concentration (1.5 nM). When SBC-5 cells were exposed to both agents simultaneously, the cell cycle pattern was between the patterns of single-agent exposure, and the size of sub-G1 fractions was substantially

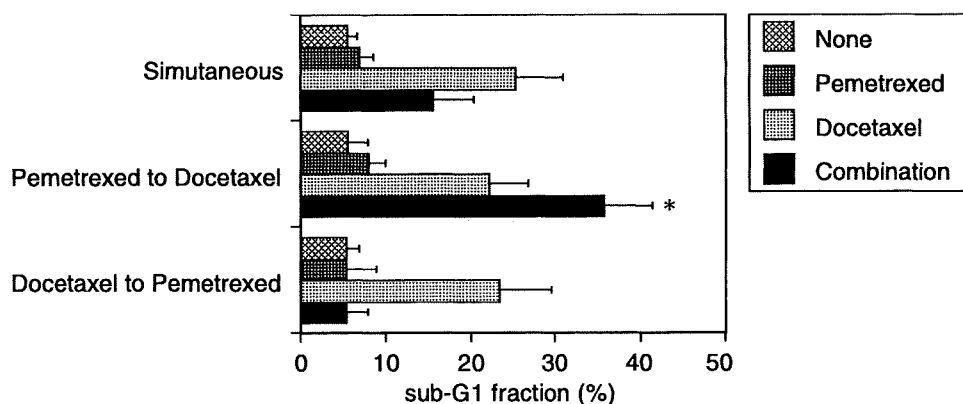
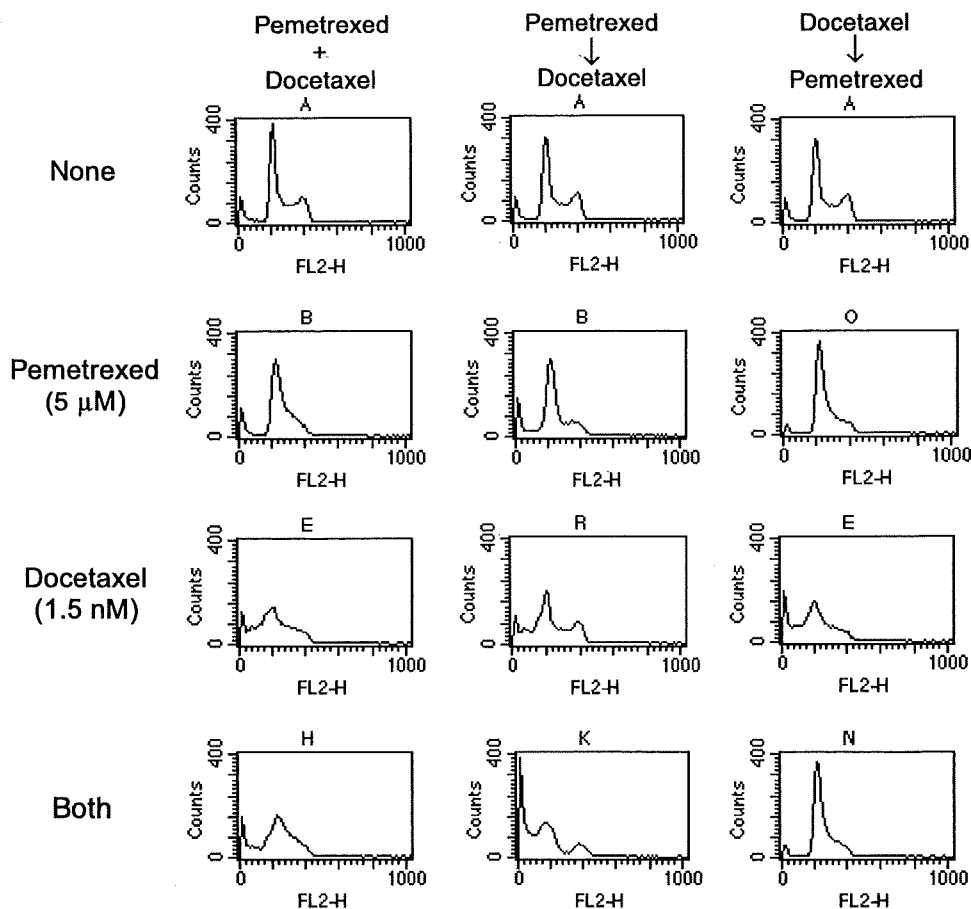


**Fig. 5** SBC-5 cells were cultured in the absence (None) or presence of either 5.0  $\mu$ M pemetrexed (Pemetrexed) or 1.5 nM docetaxel (Docetaxel) alone for 24 h; or in the presence of both drugs for 24 h (Simultaneous); or treated with pemetrexed for 24 h, followed by docetaxel for 24 h (Pemetrexed to Docetaxel); or treated with docetaxel for 24 h, followed by pemetrexed for 24 h (Docetaxel to Pemetrexed). After

72 h, DNA histograms were obtained to calculate the size of sub-G1 fractions as described in "Materials and methods". Data shown are the means  $\pm$  SD of three independent experiments. The statistical difference was determined by one-way ANOVA with Bonferroni multiple comparison test. An asterisk denotes  $P < 0.01$

**Fig. 6** Cell cycle analysis of SBC-5 cells treated with docetaxel and pemetrexed. *Left column* SBC-5 cells were treated with no drug, 5.0  $\mu$ M pemetrexed, 1.5 nM docetaxel, or both drug simultaneously for 24 h. *Middle column* SBC-5 cells were treated with 5.0  $\mu$ M pemetrexed for 24 h, followed by 1.5 nM docetaxel for 24 h. *Right column* SBC-5 cells were treated with 1.5 nM docetaxel for 24 h, followed by 5.0  $\mu$ M pemetrexed for 24 h. Cells were harvested at 72 h and DNA histogram was obtained as described in “Materials and methods”



reduced. When SBC-5 cells were treated with docetaxel first and followed by pemetrexed, the cell cycle profile was almost identical to that of single exposure to pemetrexed, suggesting that the cell cycle effect of pemetrexed is dominant over that of docetaxel. As a result, the apoptosis-inducing effect of docetaxel was almost completely cancelled in the presence of pemetrexed. In contrast, when SBC-5 cells were treated with pemetrexed first and followed by docetaxel, the proportion of cells in sub-G1 phase was larger than that of cells treated with either pemetrexed or docetaxel alone. This was accompanied by a decrease in S-phase cells. Overall, the results of cell cycle analysis are fully consistent with those of isobologram analysis, and provide the molecular basis of the sequence-dependent differences in cytotoxic interactions between the two agents.

## Discussion

In this study, we investigated the effects of pemetrexed in combination with docetaxel on lung cancer cell lines to determine the optimal schedule for this combination. Analysis of the drug–drug interaction effects was carried out

using the isobologram method of Steel and Peckham [18], which provides a fundamental basis for assessing whether cytotoxicity induced by combinations of anticancer agents is greater, equal to, or smaller than would have been expected for the individual agents.

We demonstrated that a cytotoxic interaction between pemetrexed and docetaxel is schedule-dependent. Simultaneous exposure to pemetrexed and docetaxel for 24 h and 5 days showed antagonistic effects in all cell lines studied. Sequential exposure to pemetrexed for 24 h followed by docetaxel for 24 h showed synergistic effects in Lu-99 and SBC-5 cells, while it showed additive effects in A-549 cells. Sequential exposure to docetaxel followed by pemetrexed showed additive effects in A-549 and Lu-99 cells, but antagonistic effects in SBC-5 cells. We also used SW620 colon cancer cells for the study, and the combined effects for these schedules were quite the same as those of SBC-5 cells (data not shown).

These findings suggest that the sequential administration of pemetrexed followed by docetaxel may be more cytotoxic to cancer cells and optimal for this combination, while the simultaneous administration of pemetrexed and docetaxel may be less cytotoxic and suboptimal. It should be noted that the sequential administration of pemetrexed



**Table 2** Effects of pemetrexed and docetaxel on cell cycle distribution of SBC-5 cells

Schedule	Pemetrexed + Docetaxel (%)	Pemetrexed ↓ Docetaxel (%)	Docetaxel ↓ Pemetrexed (%)
None			
Sub-G1	5.4	4.7	4.7
G1	48.4	51.3	51.3
S	24.9	22.3	22.3
G2/M	21.3	21.7	21.7
Pemetrexed (5 μM)			
Sub-G1	5.5	9.9	2.2
G1	62.8	61.6	68.2
S	28.4	18.1	20.0
G2/M	3.3	10.4	9.6
Docetaxel (1.5 nM)			
Sub-G1	25.2	17.6	21.3
G1	42.8	4.7	50.7
S	27.1	20.0	18.3
G2/M	4.9	17.7	9.7
Both			
Sub-G1	14.6	36.0	2.3
G1	52.1	40.1	66.4
S	22.7	12.2	26.0
G2/M	3.6	11.7	5.3

The proportion of cells in each phase of the cell cycle was calculated with the ModFitLT 2.0 program

followed by docetaxel might be more toxic for normal cells. Since, however, toxicity profiles of both agents are different, increasing overlapping toxicity would likely be mild.

Previously, we evaluated the cytotoxic effects of pemetrexed in combination with paclitaxel *in vitro* using A-549 cells, breast cancer MCF7, ovarian cancer PA1, and colon cancer WiDr cells *in vitro* [17]. The results were similar to those of the present study. Although slight differences are present, this would be due to the very strict definitions of synergism and antagonism in the isobologram method (Steel and Peckham). Our previous and present findings suggest that the simultaneous administration of pemetrexed and taxanes is less cytotoxic than the sequential administration of pemetrexed followed by taxanes, and latter schedule should be assessed in clinical trials for the treatment of lung cancer and other solid tumors.

In general, it is difficult to clarify the mechanisms underlying the cytotoxic effects of drug combinations. In this study, however, cell cycle analysis provided a clue to the molecular basis of schedule-dependent synergism and antagonism. The exposure of SBC-5 cells to pemetrexed led to synchronization of most cells that were in late G1 phase to the early S phase of the cell cycle, during which

cells are relatively insensitive to docetaxel. This may explain the antagonistic effects of the simultaneous addition of the two agents. In the case of sequential exposure to docetaxel followed by pemetrexed, the cell cycle pattern was almost identical to that of cells treated with pemetrexed alone. This suggests that the cell cycle effect of docetaxel is transient and overcome by the addition of pemetrexed, which results in the abrogation of its cytotoxicity.

In contrast, the sequential exposure to pemetrexed followed by docetaxel produced a striking increase in apoptotic cells along with a decrease in cells in S phase. The effect of docetaxel on S phase cells no longer in pemetrexed-induced cell cycle arrest may cause the synergistic cytotoxicity. The decrease in S phase is compatible with this notion. However, the mechanisms underlying the cytotoxic effects of pemetrexed and docetaxel are still not well understood. The possibility that the drug interactions are due to some unknown mechanism related to complex perturbations of biochemical processes cannot be excluded.

In conclusion, our data show that the antitumor activity of pemetrexed and docetaxel is schedule-dependent. Sequential exposure to pemetrexed followed by docetaxel tended to produce synergistic effects, and would therefore be a suitable schedule, whereas simultaneous exposure to the two agents had antagonistic effects, and may be suboptimal. However, the question of how far these results can be applied in the treatment of patients remains unanswered. Further clinical studies are necessary to clarify whether the therapy sequence alters the antitumor effect and the toxicity of this combination. Our findings provide preclinical rationale for a novel, mechanism-based, therapeutic strategy to be tested in lung cancer patients.

**Acknowledgment** This work was supported in part by a Grant for Third-Term-Comprehensive Control Research for Cancer from the In-Aid for Cancer Research from the Ministry of Health and Welfare of Japan.

**Conflict of interest statement** None.

## References

1. Shepherd FA (2000) Chemotherapy for advanced non-small-cell lung cancer: modest progress, many choices. *J Clin Oncol* 18(21 Suppl):35S–38S
2. Non-Small Cell Lung Cancer Collaborative Group (1995) Chemotherapy in non-small cell lung cancer: a meta analysis using updated data on individual patients from 52 randomized trials. *Br J Cancer* 311:899–909
3. Shepherd FA, Carney DN (2000) Treatment of non-small cell lung cancer: chemotherapy. In: Hansen HH (ed) *Textbook of lung cancer*. Martin Dunitz, London, pp 213–242
4. Cullen M (2006) Second-line treatment options in advanced non-small cell lung cancer: current status. *Semin Oncol* 33(1 Suppl 1):S3–S8

5. Massarelli E, Herbst RS (2006) Use of novel second-line targeted therapies in non-small cell lung cancer. *Semin Oncol* 33(1 Suppl 1):S9–S16
6. Govindan R, Page N, Morgensztern D et al (2006) Changing epidemiology of small-cell lung cancer in the United States over the last 30 years: analysis of the surveillance, epidemiologic, and end results database. *J Clin Oncol* 24:4539–4544
7. Rosti G, Carminati O, Monti M et al (2006) Chemotherapy advances in small cell lung cancer. *Ann Oncol Suppl* 5:99–102
8. Socinski MA, Weissman CH, Hart LL et al (2005) A randomized phase II trial of pemetrexed (P) plus cisplatin (cis) or carboplatin (carbo) in extensive stage small cell lung cancer (ES-SCLC). *Proc ASCO* (a 7165)
9. Gronberg BH, Bremnes RM, Aasebo U et al, on behalf of the Norwegian Lung Cancer Study Group (2008) A prospective phase II study: High-dose pemetrexed as second-line chemotherapy in small-cell lung cancer. *Lung Cancer* Jun 5 [Epub ahead of print]
10. Khan RA, Hahn B (2008) Phase II trial of weekly topotecan with docetaxel in recurrent small cell lung cancer. *Proc ASCO* (a19111)
11. Adjei AA (2004) Pemetrexed (ALIMTA), a novel multitargeted antineoplastic agent. *Clin Cancer Res* 10:4276S–4280S
12. Hanna N, Shepherd FA, Fossella FV et al (2004) Randomized phase III trial of pemetrexed versus docetaxel in patients with non-small-cell lung cancer previously treated with chemotherapy. *J Clin Oncol* 22:1589–1597
13. Shih C, Chen VJ, Gossett LS et al (1997) LY231514, a pyrrolo[2,3-d]pyrimidine-based antifolate that inhibits multiple folate-requiring enzymes. *Cancer Res* 57:1116–1123
14. Tonkinson JL, Marder P, Andis SL et al (1997) Cell cycle effects of antifolate antimetabolites: implications for cytotoxicity and cytostasis. *Cancer Chemother Pharmacol* 39:521–531
15. Jones SE, Erban J, Overmoyer B et al (2005) Randomized phase III study of docetaxel compared with paclitaxel in metastatic breast cancer. *J Clin Oncol* 23:5542–5551
16. Gligorov J, Lotz JP (2004) Preclinical pharmacology of the taxanes: implications of the differences. *Oncologist* 9(Suppl 2):3–8
17. Kano Y, Akutsu M, Tsunoda S et al (2004) Schedule-dependent synergism and antagonism between pemetrexed and paclitaxel in human carcinoma cell lines in vitro. *Cancer Chemother Pharmacol* 54:505–513
18. Steel GG, Peckham MJ (1979) Exploitable mechanisms in combined radiotherapy-chemotherapy: the concept of additivity. *Int J Radiat Oncol Biol Phys* 5:85–91
19. Kano Y, Sakamoto S, Kasahara T et al (1991) In vitro effects of amsacrine in combination with other anticancer agents. *Leukemia Res* 15:1059–1064
20. Kano Y, Ohnuma T, Okano T et al (1988) Effects of vincristine in combination with methotrexate and other antitumor agents in human acute lymphoblastic leukemia cells in culture. *Cancer Res* 48:351–356
21. Kano Y, Suzuki K, Akutsu M et al (1992) Effects of CPT-11 in combination with other anticancer agents in culture. *Int J Cancer* 50:604–610
22. Kano Y, Akutsu M, Tsunoda S et al (1994) In vitro schedule-dependent interaction between and SN-38 (the active metabolite of irinotecan) in human carcinoma cell lines. *Cancer Chemother Pharmacol* 42:91–98
23. Kikuchi J, Shimizu R, Wada T et al (2007) E2F-6 suppresses growth-associated apoptosis of human hematopoietic progenitor cells by counteracting proapoptotic activity of E2F-1. *Stem Cells* 25:2439–2447

## The Cytotoxic Effects of Gemtuzumab Ozogamicin (Mylotarg) in Combination with Conventional Antileukemic Agents by Isobologram Analysis *In Vitro*

MASARU TANAKA<sup>1</sup>, YASUHIKO KANO<sup>1</sup>, MIYUKI AKUTSU<sup>1</sup>, SABURO TSUNODA<sup>1</sup>, TOHRU IZUMI<sup>1</sup>, YASUO YAZAWA<sup>2</sup>, SHUICH MIYAWAKI<sup>3</sup>, HIROYUKI MANO<sup>4</sup> and YUSUKE FURUKAWA<sup>5</sup>

*Divisions of*<sup>1</sup>*Hematology and*<sup>2</sup>*Orthopedic Oncology, Tochigi Cancer Center, Tochigi;*  
<sup>3</sup>*Leukemia Research Center, Saiseikai Maebashi Hospital, Gunma;*  
*Divisions of*<sup>4</sup>*Functional Genomics and*<sup>5</sup>*Stem Cell Regulation,*  
*Center for Molecular Medicine, Jichi Medical University, Tochigi, Japan*

**Abstract.** *Background: The CD33 antigen is expressed on leukemia cells in most patients with acute myeloid leukemia (AML) and acute promyelocytic leukemia (APL), and in 20% of patients with acute lymphoblastic leukemia (ALL), while it is absent from pluripotent hematopoietic stem cells and nonhematopoietic cells. Gemtuzumab ozogamicin (GO) is an immunconjugate of an anti-CD33 antibody linked to calicheamicin, which is a potent cytotoxic agent that causes double-strand DNA breaks, resulting in cell death. GO was developed against CD33 antigen-positive leukemias. The aim of this study was to investigate the cytotoxic effects of this agent in combination with conventional antileukemic agents. Materials and Methods: The cytotoxic effects of GO in combination with antileukemic agents were studied against human CD33 antigen-positive leukemia HL-60, U937, TCC-S and NALM20 cells. The leukemia cells were exposed simultaneously to GO and to the other agents for 4 days. Cell growth inhibition was determined using a MTT reduction assay. The isobologram method was used to evaluate the cytotoxic interaction. Results: GO produced synergistic effects with mitoxantrone, additive effects with cytarabine, daunorubicin, idarubicin, doxorubicin, etoposide and 6-mercaptopurine, and antagonistic effects with methotrexate and vincristine. Conclusion: Our findings suggest that the simultaneous administration of GO with most agents studied would be advantageous for antileukemic activity. The simultaneous administration of GO with methotrexate or*

*vincristine would have little cytotoxic effect, and this combination may be inappropriate. These findings may be useful in clinical trials of combination chemotherapy including GO or other monoclonal antibodies linked to calicheamicin.*

Gemtuzumab ozogamicin (GO) is a humanized anti-CD33 antibody conjugated with the cytotoxic antibiotic calicheamicin (1, 2), which is a potent chemotherapeutic agent with a low therapeutic index that requires targeting to tumor cells for clinical use. On binding to target cells, the antibody-antigen complex is internalized into the cells, and hydrolytic release of the toxic calicheamicin moiety occurs, which subsequently causes DNA double-strand breaks that lead to apoptosis (1, 3, 4).

Acute myeloid leukemia (AML) is a major target of GO, since the CD33 antigen is expressed on blast cells in most patients with AML, while it is absent from pluripotent hematopoietic stem cells and nonhematopoietic cells (5-8). In spite of positive expectations, GO only has a moderate antileukemic activity. It produces a complete response (CR) rate of 10-16% of cases, with another 7-15% achieving CR with inadequate platelet recovery in relapsed CD33-positive AML (9-16). The median survival of patients treated with GO alone is less than 6 months. GO in monotherapy at 9 mg/m<sup>2</sup> is complicated by hepatic veno-occlusive disease in 5-10% of patients. Acute promyelocytic leukemia (APL) cells express large amounts of CD33 and GO is also effective as a single agent with relapsed APL, including those cases with very advanced disease (17).

Around 20% of acute lymphoblastic leukemia (ALL) is also observed to express CD33 and is considered as a target of GO (5-8). Preclinical studies have shown that CD33-positive ALL cells are much more sensitive to GO than are AML cells (18). In clinical studies, several cases of relapsed CD33-positive ALL were reported to achieve complete remission following GO administration (19-20).

*Correspondence to:* Dr. Yusuke Furukawa, Stem Cell Regulation, Center for Molecular Medicine, Jichi Medical University, 3311-Yakushiji, Shimotsuke, Tochigi, 329-0498, Japan. Tel: +81285587400, Fax: +81285587501, e-mail: furuyu@jichi.ac.jp

**Key Words:** Gemtuzumab, calicheamicin, isobologram, CD33, leukemia.

Combination of lower doses of GO with other agents is the next strategy for improving the response and avoiding toxicity, and clinical studies are in progress for fresh and relapsed AML, APL and CD33-positive ALL cases as remission induction and consolidation therapies with other agents with a variety of schedules (15, 16, 21-26). However, to our knowledge, there are no experimental data available about the cytotoxic effects of GO in combination with conventional antileukemic agents. In the present study, we investigated the *in vitro* effects of GO in combination with antileukemia agents against CD33-positive human leukemia cell lines.

**Materials and Methods**

**Cell lines.** Experiments were conducted with CD33-positive human acute myeloid leukemias, U937 and HL-60, and Philadelphia chromosome-positive myeloid leukemia TCC-S, and acute lymphoblastic leukemia NALM20 cells. HL-60 and U937 were obtained from Health Science Research Resources Bank (Osaka, Japan). TCC-S was established in our laboratory (27). NALM20 was kindly donated by Yoshinobu, Matsuo, Hayashibara Biochemical Laboratories Inc., Fujisaki Cell Centre (Okayama, Japan). Cells were maintained in 75-cm<sup>3</sup> plastic tissue culture flasks containing RPMI-1640 medium (Sigma, St. Louis, MO, USA) supplemented with 10% heat-inactivated fetal bovine serum (FBS) (Grand Island Biological Co. Grand Island, NY, USA) and antibiotics. The cell cycle times of rapidly growing U937, HL60 and TCC-S cells were around 24 h, while that of slowly growing NALM20 cells was 70-80 h.

**Drugs.** Anticancer agents used and their sources were: GO (Wyeth Laboratories, Philadelphia, PA, USA), cytarabine (Nihon Shinyaku Co. Ltd., Tokyo, Japan), daunorubicin (Meiji Co. Ltd., Tokyo, Japan), doxorubicin (Meiji Co. Ltd., Tokyo, Japan), idarubicin (Pfizer Japan Inc. Tokyo, Japan), etoposide (Nihon Kayaku Co. Ltd., Tokyo, Japan), 6-mercaptopurine (Takeda Co. Ltd., Tokyo, Japan), vincristine (Shionogi Co. Ltd., Tokyo, Japan), and methotrexate (Wyeth Lederle Japan Ltd., Tokyo, Japan). All drugs were dissolved in RPMI-1640. Appropriate drug concentrations were made by dilution with fresh medium immediately before each experiment.

**Inhibition of cell growth by combination of GO and other agents.** Two to four leukemia cell lines were used for the each study of GO in combination with other agents. Leukemia cells lines were harvested from the media and resuspended to a final density of 1×10<sup>5</sup> cells/ml for U937, HL-60, and TCC-S cells, and of 5×10<sup>5</sup> cells/ml for NALM20. Cell suspensions (100 μl) were dispensed into individual wells of 96-well tissue culture plates with lids (Falcon, Oxnard, CA, USA). Eight plates were prepared for the testing of each drug combination. Each plate had one 8-well control column containing medium alone and one 8-well control column containing cells but no drugs. Cells were incubated in a humidified atmosphere of 95% air/5% CO<sub>2</sub> at 37°C overnight. Drug solutions of GO and other drugs at different concentrations were then added (50 μl) to 8 wells containing cell suspensions and the plates were then incubated under the same conditions for 4 days for U937, HL-60 and TCC-S cells, and for 8 days for NALM20 cells.

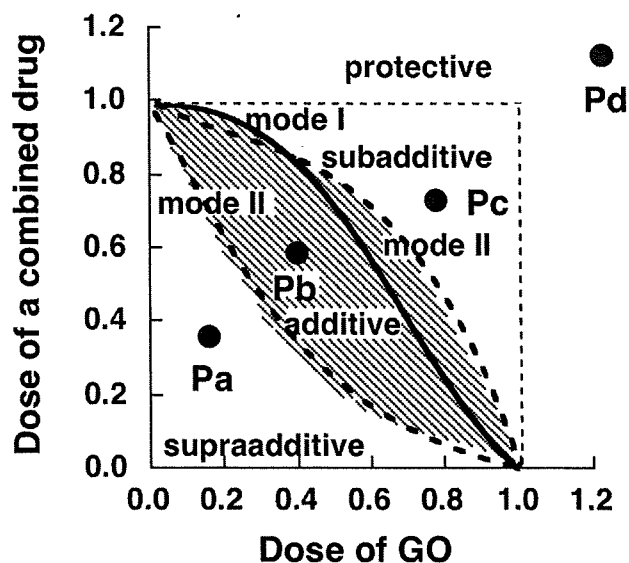


Figure 1. Schematic representation of isobologram. Envelope of additivity (shaded area), surrounded by mode I (solid line) and mode II (dotted lines) isobologram lines, was constructed from the dose-response curves (shaded area) of GO and a combined drug. The concentrations that produced 80% cell growth inhibition were expressed as 1.0 on the ordinate and the abscissa of the isobolograms. Combined data points Pa, Pb, Pc, and Pd show supraadditive, additive, subadditive, and protective effects, respectively.

**3-(4,5-Dimethylthiazol-2-yl)-2,5-diphenyltetrazolium bromide assay (MTT assay).** Viable cell growth was determined using a modified MTT assay as described previously (28).

**Isobologram method of Steel and Peckham.** Cytotoxic interactions of GO with other agents at the 80% inhibitory concentration (IC<sub>80</sub>) level were evaluated by the isobologram method of Steel and Peckham (Figure 1) (29). The theoretical basis of the isobologram method and the procedure for making isobolograms have been described in detail previously (30, 31).

Based upon the dose-response curves of GO and the other agents, three isoeffect curves were constructed (Figure 1). If the agents were acting additively by independent mechanisms, the combined data points would lie near the mode I line (hetero-addition). If the agents were acting additively by similar mechanisms, the combined data points would lie near the mode II lines (iso-addition).

Since it is unknown in advance whether the combined effects of two agents will be hetero-additive, iso-additive or an effect intermediate between these extremes, all possibilities should be considered. Thus, when the data points of the drug combination fell within the area surrounded by three lines (envelope of additivity), the combination was regarded as additive. When the data points fell to the left of the envelope, *i.e.* the combined effect was caused by lower doses of the two agents than was predicted, we regarded the drug combination as having a supraadditive effect (synergism). When the points fell to the right of the envelope, *i.e.* the combined effect was caused by higher doses of the two agents than was predicted, but within the square or on the line of the square, we regarded the combination as having a subadditive effect, *i.e.* the combination was

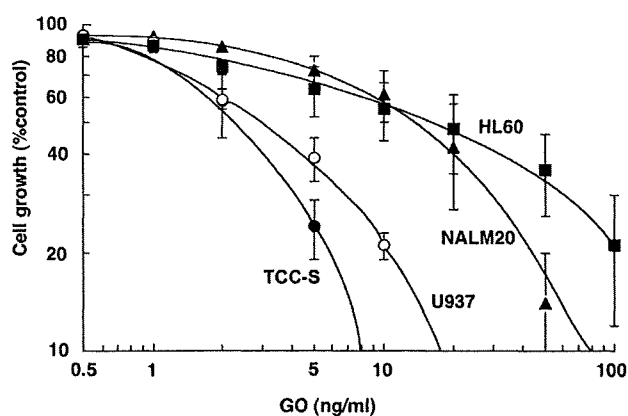


Figure 2. The dose-response curves of GO in U937, HL-60, TCC-S and NALM20 cells. Cell growth inhibition was measured using the MTT assay and was plotted as a percentage of the control (cells not exposed to drugs). Each point represents the mean  $\pm$  SEM ( $n > 10$ ).

superior or equal to the single agents but was less than additive. When the data points were outside the square, the combination was regarded as having a protective effect, *i.e.* the combination was inferior in cytotoxic action to the single agents. Both subadditive and protective interactions were regarded as antagonism.

**Data analysis.** To determine whether the condition of synergism (or antagonism) truly existed, statistical analysis was performed. The Wilcoxon signed-ranks test was used for comparing the observed data with the predicted minimum (or maximum) values for additive effects, which were closest to the observed data (*i.e.* the data on the boundary (mode I or mode II lines) between the additive area and supraadditive area (or subadditive and protective areas) (32). Probability ( $P$ ) values  $\leq 0.05$  were considered to be significant. Combinations with  $p > 0.05$  were regarded as indicating additive/synergistic (or additive/antagonistic) effects. All statistical analyses were performed using the Stat View 4.01 software program (Abacus Concepts, Berkeley, CA, USA).

## Results

Figure 2 shows the dose-response curves of GO in U937, HL-60, TCC-S and NALM20 cells. The  $IC_{80}$  values of GO alone against U937, HL-60, TCC-S, and NALM20 cells were  $10.9 \pm 1.1$  ng/ml,  $100 \pm 36$  ng/ml,  $5.6 \pm 1.1$  ng/ml, and  $41 \pm 9$  ng/ml, respectively ( $n > 10$ ). Figure 3 shows the dose-response curves for GO in combination with cytarabine, doxorubicin, and vincristine in U937 cells. Each isobologram was generated based on such dose-response curves.

**Cytotoxic effects of GO in combination with cytarabine.** U937, HL-60 and TCC-S cells were used for this combination study. Figure 4A-C shows the isobolograms of the combination of GO and cytarabine in these cells. In the U937 cells, the combined data points fell within the envelope of additivity (Figure 4A). The mean value of the data (0.55)

was larger than that of the predicted minimum value (0.39) and smaller than that of the predicted maximum value for an additive effect (0.74) (Table I), indicating that the simultaneous exposure to GO and cytarabine produced an additive effect. In HL-60 and TCC-S cells, most data points for the combination also fell within the envelope of additivity (Figure 4B, and C). These findings suggest that the simultaneous administration of GO and cytarabine produced additive effects.

**Cytotoxic effects of GO in combination with doxorubicin, daunorubicin, idarubicin, or etoposide.** Figure 5A-C shows the isobolograms of the combination of GO with doxorubicin in U937, HL-60 and TCC-S cells, respectively. In all cell lines, all combined data points fell within the envelope of additivity, indicating that the simultaneous exposure to GO and doxorubicin produced additive effects (Table I). The simultaneous exposure to GO and daunorubicin, idarubicin, and etoposide showed quite similar effects (isobolograms not shown) in the cell lines studied (Table I)

**Cytotoxic interaction between GO and mitoxantrone.** U937 and HL60 cells were used for this study and showed similar effects. Most data points for the combination fell in the area of supraadditivity (isobolograms not shown). The mean values of the data were slightly smaller than those of the predicted minimum values for an additive effect (Table I). Statistical analysis showed that the difference was significant, indicating that the simultaneous exposure to GO and mitoxantrone produced marginally synergistic effects.

**Cytotoxic effects of GO in combination with 6-mercaptopurine.** U937, HL60 and TCC-S cells were used for this study. U937 and TCC-S cells were resistant to 6-mercaptopurine and the cytotoxic effects of this combination were evaluated at the  $IC_{50}$  level. In all three cell lines studied, most combined data points fell within the envelope of additivity, indicating that the simultaneous exposure to GO and 6-mercaptopurine produced additive effects (Table I).

**Cytotoxic interaction between GO and methotrexate.** In all four cell lines studied, most data points for the combination fell in the areas of sub-additivity and protection (isobolograms not shown). The mean values of the observed data were larger than those of the predicted maximum additive values (Table I). The difference was statistically significant, indicating antagonistic effects of the simultaneous exposure to these two agents.

**Cytotoxic interaction between GO and vincristine.** All four cell lines were used for this study. Figure 6A-C shows the isobolograms of this combination of this combination in U937, HL-60, and TCC-S cells, respectively. In U937, TCC-

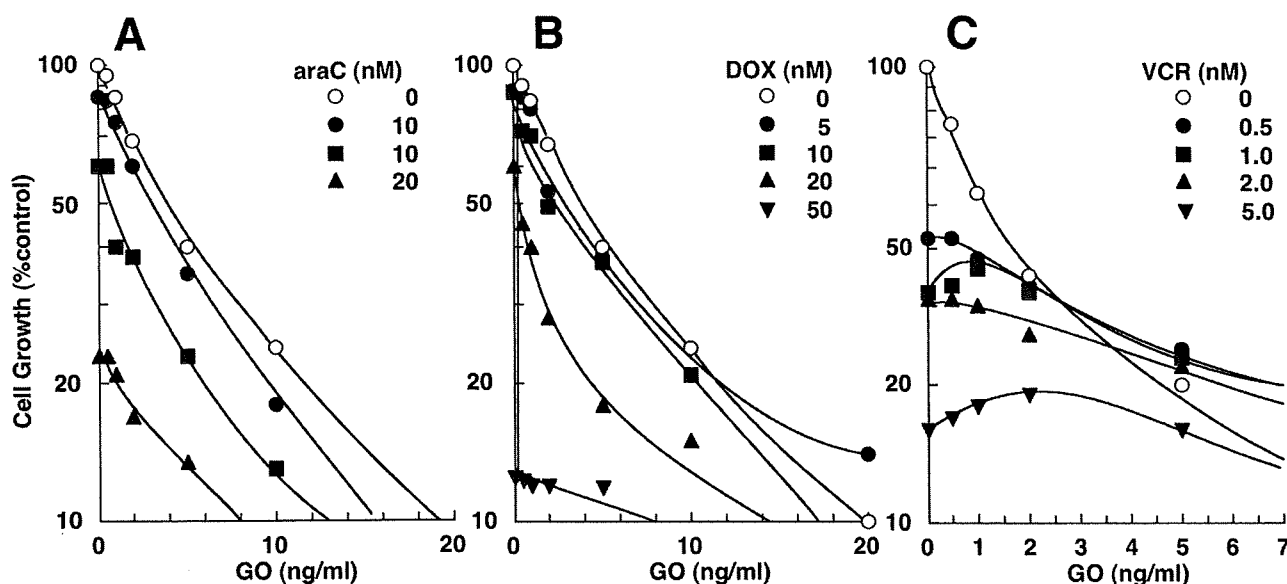


Figure 3. Dose-response curves for GO in combination with cytarabine (ara-C) (A), doxorubicin (DOX) (B) and vincristine (VCR) (C) in U937 cells. Cell growth was measured using the MTT assay after 4 days and was plotted as a percentage of the control (cells not exposed to drugs). Each point represents the mean value for at least three independent experiments; the SEs of the means were less than 25% and are thus omitted.

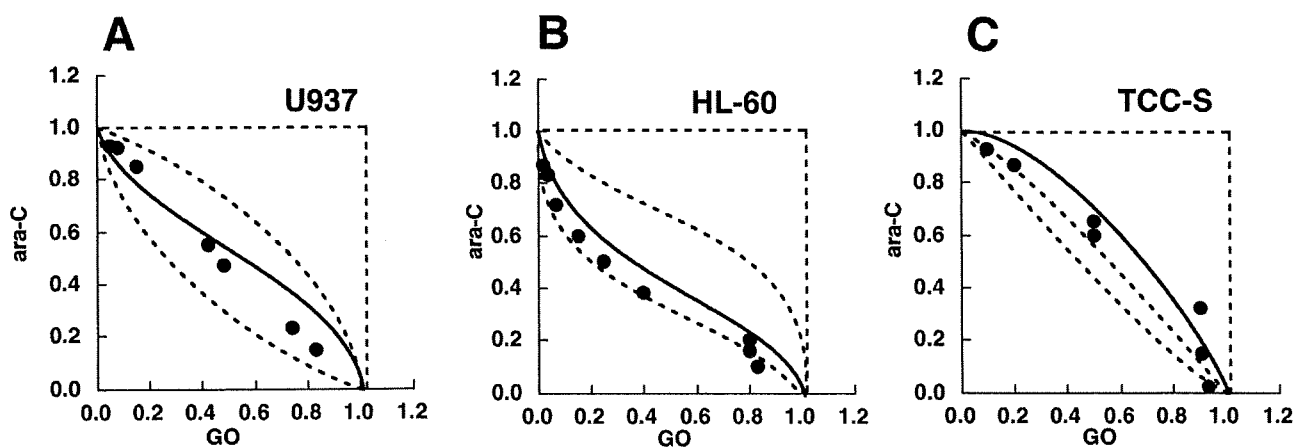


Figure 4. Isobolograms of simultaneous exposure to GO and cytarabine (ara-C) in U937 (A), HL-60 (B) and TCC-S (C) cells. Data are presented as mean values of at least three independent experiments. In all three cell lines, all or most data points of the combinations fell within the envelope of additivity, suggesting additive interactions.

S and NALM20 cells, the data points fell in the areas of subadditivity and protection. The mean values of the observed data were larger than those of the predicted maximum additive values. Statistical analysis showed that the difference was significant, indicating antagonistic effects (Table I). For HL60 cells, the data points fell within the envelope of additivity and in the area of subadditivity. The mean value of the observed data was slightly smaller than that of the predicted maximum additive value, indicating additive effects.

### Discussion

Linking anticancer agents to an antibody that recognizes a tumor-associated antigen can improve the therapeutic index of the drug. The most promising results have been obtained with GO ozogamicin, a CD33 monoclonal antibody joined to the potent cytotoxin calicheamicin. The purpose of this study was to assess the cytotoxic effects of GO alone or in combination with commonly used antileukemic agents against CD33-positive leukemia cell lines.

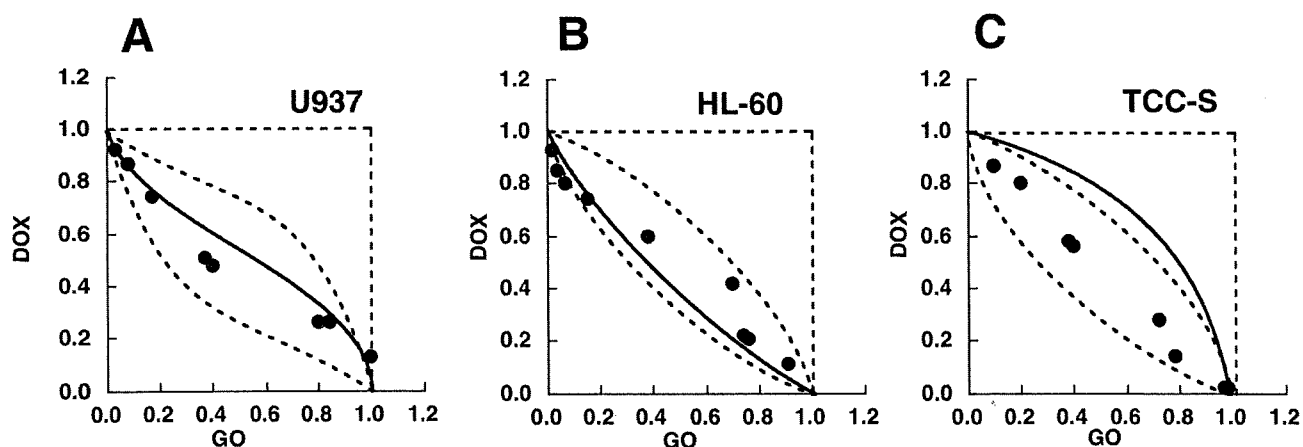


Figure 5. Isobolograms of simultaneous exposure to GO and doxorubicin (DOX) in U937 (A), HL-60 (B) and TCC-S (C) cells. Data are presented as mean values of at least three independent experiments. In all three cell lines, all or most data points of the combinations fell within the envelope of additivity, suggesting additive interactions.

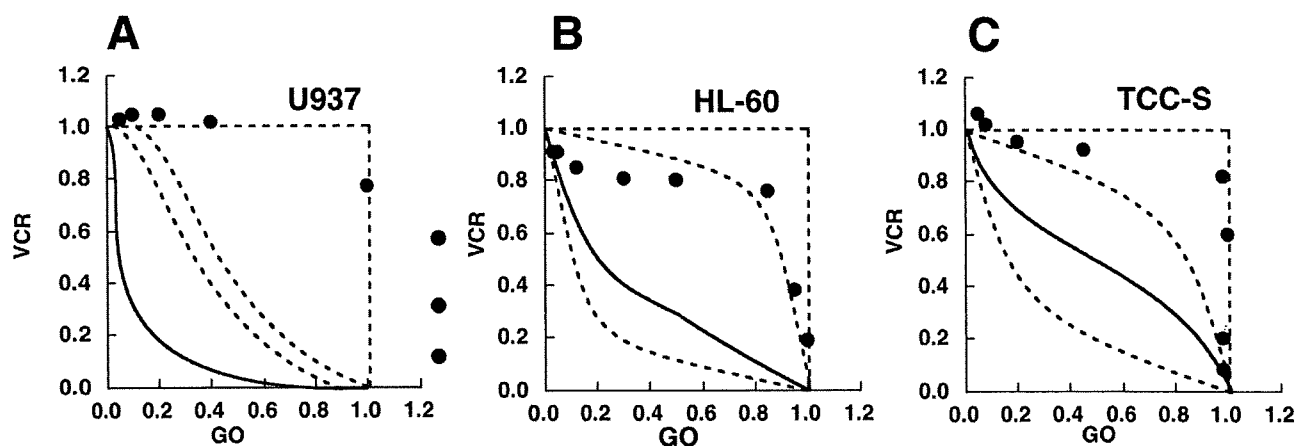


Figure 6. Isobolograms of simultaneous exposure to GO and vincristine (VCR) in U937 (A), HL-60 (B) and TCC-S (C) cells. Data are presented as mean values of at least three independent experiments. In U937 and TCC-S lines, all or most data points fell in the areas of sub-additivity and protection, suggesting antagonistic interactions, while, in HL-60 cells, data points of the combinations fell within the envelope of additivity and in the area of subadditivity, suggesting additive interactions.

The  $IC_{80}$  values of GO alone against U937, HL-60, TCC-S and NALM20 cells were approximately 10 ng/ml, 100 ng/ml, 5 ng/ml and 10 ng/ml, respectively. From the pharmacokinetic study, these concentrations are clinically achievable as the peak plasma concentration of GO was  $2.86 \pm 1.35$  mg/l and the half life of GO was  $72.4 \pm 42.0$  h after administration of the first  $9 \text{ mg/m}^2$  dose of GO (33).

We studied the cytotoxic effects of GO in combination with conventionally used antileukemic agents. Cytarabine and anthracyclines such as daunorubicin and idarubicin are most widely used for remission induction or consolidation therapy of AML. At present, clinical trials of remission induction or consolidation therapy, with or without GO, are

in progress. In our study, GO in combination with cytarabine and anthracyclines showed additive effects for all three cell lines studied.

The combination of cytarabine and an anthracenedione anticancer agent, mitoxantrone, is also used for the treatment of AML. Both anthracyclines and mitoxantrone inhibit topoisomerase-II and disrupt DNA synthesis and DNA repair in cancer cells. Mitoxantrone produced marginally synergistic effects with GO. These findings suggest that the simultaneous administration of GO with cytarabine or topoisomerase-II inhibitors could produce the expected (or more than expected) clinical activity. However, since the dose-limiting toxicity of GO, cytarabine, and topoisomerase-

Table I. Mean values of observed data, predicted minimum, and predicted maximum of gemtuzumab ozogamicin in combination with other anticancer agents.

Combined drug	Cell line	No. of data points	Observed data*	Predicted min.**	Predicted max.***	Effect
Cytarabine	U937	6	0.55	0.39	0.74	Additive
	HL60	9	0.67	0.49	0.85	Additive
	TCC-S	7	0.81	0.67	0.83	Additive
Doxorubicin	U937	8	0.68	0.50	0.84	Additive
	HL60	9	0.67	0.49	0.85	Additive
	TCC-S	8	0.74	0.58	0.91	Additive
Daunorubicin	NALM-20	9	0.67	0.64	0.81	Additive
	U937	6	0.66	0.49	0.86	Additive
	HL60	5	0.47	0.32	0.70	Additive
Idarubicin	U937	7	0.63	0.56	0.84	Additive
	HL60	6	0.51	0.37	0.81	Additive
Mitoxantrone	U937	6	0.54	0.60	0.82	Synergism ( $p < 0.05$ )
	HL60	7	0.51	0.57	0.68	Synergism ( $p < 0.05$ )
Etoposide	U937	7	0.53	0.51	0.63	Additive
	HL60	9	0.60	0.56	0.79	Additive
	TCC-S	7	0.53	0.49	0.75	Additive
6-Mercaptopurine	U937	7	0.66	0.60	0.69	Additive ( $IC_{50}$ )
	HL60	7	0.54	0.46	0.66	Additive
	TCC-S	5	0.52	0.53	0.58	Additive ( $IC_{50}$ )
Methotrexate	U937	6	>1.19	0.23	0.84	Antagonism ( $p < 0.01$ )
	HL60	7	0.92	0.23	0.81	Antagonism ( $p < 0.05$ )
	TCC-S	7	0.81	0.05	0.40	Antagonism ( $p < 0.02$ )
	NALM-20	9	0.86	0.32	0.75	Antagonism ( $p < 0.01$ )
Vincristine	U937	8	>1.09	0.26	0.66	Antagonism ( $p < 0.01$ )
	HL60	8	0.90	0.36	0.93	Additive
	TCC-S	10	0.97	0.36	0.87	Antagonism ( $p < 0.01$ )
	NALM-20	9	0.91	0.40	0.85	Antagonism ( $p < 0.05$ )

\*Mean value of observed data; \*\*mean value of the predicted minimum values for an additive effect; \*\*\*mean value of predicted maximum values for an additive effect.

If inhibitors involves myelosuppression, there must be careful monitoring for myelosuppression during the combination treatment.

About 20% of ALL is observed to express CD33 and is considered as a target of GO (5-8) and encouraging data have been obtained from preclinical and clinical studies (18-20). Recently, a CD22-targeted immunoconjugate of calicheamicin (CMC-544) has been developed for B-cell non-Hodgkin's lymphoma and ALL. CMC-544 has shown significant preclinical potential in studies in a mouse model (34-36).

We also studied the cytotoxic effects of GO in combination with methotrexate and vincristine, which are mainly used for lymphoid malignancies. GO showed definite antagonistic effects with methotrexate and vincristine in four out of four, and three out of four cell lines, respectively (Table I). The observed data values of GO in combination with methotrexate and vincristine were greater than 0.80 in all cell lines. These combinations also produced protective effects in the Philadelphia chromosome-positive leukemia cell line KU812 (data, not shown). Our findings suggest that the simultaneous

administration of GO with methotrexate or vincristine may have almost no cytotoxic advantage over the administration of either agent alone, and thus may be inappropriate for the treatment of CD33-positive ALL. When CMC-544 is clinically available, the simultaneous administration of CMC-544 with methotrexate or vincristine would be also inappropriate.

There are a number of difficulties in the translation of results from *in vitro* to clinical therapy, and the pharmacokinetic profiles are significantly different between them. The toxic effects of the combination cannot be measured by *in vitro* systems, and the cell kinetics and cell biochemistry may be quite different. These differences between *in vitro* and clinical systems may influence the cytotoxic interaction of GO and other agents. In addition, we tested only simultaneous exposure to GO and other agents. Since cytotoxic effects are often schedule dependent, sequential exposure to GO followed by other agents or the reverse sequence may not show the same effects as simultaneous exposure to these agents. Continued preclinical and clinical studies would be necessary to assist in determining the optimal combination and schedule of GO in clinical use.



In conclusion, the present study suggests that the simultaneous administration of GO with most agents studied would be advantageous for antileukemic activity. The simultaneous administration of GO with methotrexate or vincristine would have little cytotoxic effect, and these combinations may be inappropriate. Our findings may be useful in clinical trials of combination chemotherapy including GO or other monoclonal antibodies linked to calicheamicin.

## Disclosure

No disclosures.

## Conflict of Interest

The authors declare that they have no potential conflicts of interest.

## Acknowledgements

The study was partially supported by a Grant in Aid (No.13204075) from the Japanese Ministry of Education, Culture, Sports, Science and Technology of Japan.

## References

- 1 Zein N, Sinha AM, McGahren WJ and Ellestad GA: Calicheamicin gamma II: an antitumor antibiotic that cleaves double-stranded DNA site specifically. *Science* 240(4856): 1198-1201, 1988.
- 2 Sievers EL, Appelbaum FR, Spielberger RT, Forman SJ, Flowers D, Smith FO, Shannon-Dorcy K, Berger MS and Bernstein ID: Selective ablation of acute myeloid leukemia using antibody-targeted chemotherapy: a phase I study of an anti-CD33 calicheamicin immunconjugate. *Blood* 93: 3678-3684, 1999.
- 3 Hinman LM, Hamann PR, Wallace R, Menendez AT, Durr FE and Upeslaci J: Preparation and characterization of monoclonal antibody conjugates of the calicheamicins: a novel and potent family of antitumor antibiotics. *Cancer Res* 53: 3336-3342, 1993.
- 4 Jedema I, Barge RM, van der Velden VH, Nijmeijer BA, van Dongen JJ, Willemze R and Falkenburg JH: Internalization and cell cycle-dependent killing of leukemic cells by gemtuzumab ozogamicin: rationale for efficacy in CD33-negative malignancies with endocytic capacity. *Leukemia* 18: 316-325, 2004.
- 5 Griffin JD, Linch D, Sabbath K, Larcom P and Schlossman SF: A monoclonal antibody reactive with normal and leukemic human myeloid progenitor cells. *Leuk Res* 8: 521-534, 1984.
- 6 Dinndorf PA, Andrews RG, Benjamin D, Ridgway D, Wolff L and Bernstein ID: Expression of normal myeloid-associated antigens by acute leukemia cells. *Blood* 67: 1048-1053, 1986.
- 7 Scheinberg DA, Tanimoto M, McKenzie S, Strife A, Old LJ and Clarkson BD: Monoclonal antibody M195: a diagnostic marker for acute myelogenous leukemia. *Leukemia* 3: 440-445, 1989.
- 8 Terstappen LW, Safford M, Konemann S, Loken MR, Zurlutter K, Buchner T, Hiddemann W and Wormann B: Flow cytometric characterization of acute myeloid leukemia. Part II. Phenotypic heterogeneity at diagnosis. *Leukemia* 6: 70-80, 1992.
- 9 Sievers EL, Larson RA, Stadtmauer EA, Estey E, Lowenberg B, Dombret H, Karanes C, Theobald M, Bennett JM, Sherman ML, Berger MS, Eten CB, Loken MR, van Dongen JJ, Bernstein ID and Appelbaum FR; Mylotarg Study Group: Efficacy and safety of gemtuzumab ozogamicin in patients with CD33-positive acute myeloid leukemia in first relapse. *J Clin Oncol* 19: 3244-3254, 2001.
- 10 Larson RA, Boogaerts M, Estey E, Karanes C, Stadtmauer EA, Sievers EL, Mineur P, Bennett JM, Berger MS, Eten CB, Munteanu M, Loken MR, Van Dongen JJ, Bernstein ID and Appelbaum FR; Mylotarg Study Group: Antibody-targeted chemotherapy of older patients with acute myeloid leukemia in first relapse using Mylotarg (gemtuzumab ozogamicin). *Leukemia* 16: 1627-1636, 2002.
- 11 Piccaluga PP, Martinelli G, Rondoni M, Malagola M, Gaitani S, Isidori A, Bonini A, Gugliotta L, Luppi M, Morselli M, Sparaventi G, Visani G and Baccarani M: Gemtuzumab ozogamicin for relapsed and refractory acute myeloid leukemia and myeloid sarcomas. *Leuk Lymphoma* 45: 1791-1795, 2004.
- 12 Larson RA, Sievers EL, Stadtmauer EA, Lowenberg B, Estey EH, Dombret H, Theobald M, Voliotis D, Bennett JM, Richie M, Leopold LH, Berger MS, Sherman ML, Loken MR, van Dongen JJ, Bernstein ID and Appelbaum FR: Final report of the efficacy and safety of gemtuzumab ozogamicin (Mylotarg) in patients with CD33-positive acute myeloid leukemia in first recurrence. *Cancer* 104: 1442-1452, 2005.
- 13 Amadori S, Suci S, Stasi R, Willemze R, Mandelli F, Selleslag D, Denzlinger C, Muus P, Stauder R, Berneman Z, Pruijt J, Nobile F, Cassibba V, Marie JP, Beeldens F, Baila L, Vignetti M and de Witte T: Gemtuzumab ozogamicin (Mylotarg) as single-agent treatment for frail patients 61 years of age and older with acute myeloid leukemia: final results of AML-15B, a phase 2 study of the European Organisation for Research and Treatment of Cancer and Gruppo Italiano Malattie Ematologiche dell'Adulto Leukemia Groups. *Leukemia* 19: 1768-1773, 2005.
- 14 Nabhan C, Rundhaugen LM, Riley MB, Rademaker A, Boehlke L, Jatoi M and Tallman MS: Phase II pilot trial of gemtuzumab ozogamicin (GO) as first-line therapy in acute myeloid leukemia patients age 65 or older. *Leuk Res* 29: 53-57, 2005.
- 15 Tsimberidou AM, Giles FJ, Estey E, O'Brien S, Keating MJ and Kantarjian HM: The role of gemtuzumab ozogamicin in acute leukaemia therapy. *Br J Haematol* 132: 398-409, 2006.
- 16 Stasi R, Evangelista ML, Buccisano F, Venditti A and Amadori S: Gemtuzumab ozogamicin in the treatment of acute myeloid leukemia. *Cancer Treat Rev* 34: 49-60, 2008.
- 17 Lo-Coco F, Cimino G, Breccia M, Noguera NI, Diverio D, Finolezzi E, Pogliani EM, Di Bona E, Micalizzi C, Kropp M, Venditti A, Tafuri A and Mandelli F: Gemtuzumab ozogamicin (Mylotarg) as a single agent for molecularly relapsed acute promyelocytic leukemia. *Blood* 104: 1995-1999, 2004.
- 18 Lucio P, Gaipa G, van Lochem EG, van Wering ER, Porwit-MacDonald A, Faria T, Bjorklund E, Biondi A, van den Beemd MW, Baars E, Vidriales B, Parreira A, van Dongen JJ, San Miguel JF and Orfao A; BIOMED-I concerted action report: flow cytometric immunophenotyping of precursor B-ALL with standardized triple-stainings. BIOMED-1 Concerted Action Investigation of Minimal Residual Disease in Acute Leukemia: International Standardization and Clinical Evaluation. *Leukemia* 15: 1185-1192, 2001.

- 19 Cotter M, Rooney S, O'Marcaigh A and Smith OP: Successful use of gemtuzumab ozogamicin in a child with relapsed CD33-positive acute lymphoblastic leukaemia. *Br J Haematol* 122: 687-688, 2003.
- 20 Zwaan CM, Reinhardt D, Jurgens H, Huismans DR, Hahlen K, Smith OP, Biondi A, van Wering ER, Feingold J and Kaspers GJ: Gemtuzumab ozogamicin in pediatric CD33-positive acute lymphoblastic leukemia: first clinical experiences and relation with cellular sensitivity to single-agent calicheamicin. *Leukemia* 17: 468-470, 2003.
- 21 Amadori S, Suci S, Willemze R, Mandelli F, Selleslag D, Stauder R, Ho A, Denzlinger C, Leone G, Fabris P, Muus P, Vignetti M, Hagemeyer A, Beeldens F, Anak O and De Witte T; EORTC leukemia group; GIMEMA leukemia group: Sequential administration of gemtuzumab ozogamicin and conventional chemotherapy as first-line therapy in elderly patients with acute myeloid leukemia: a phase II study (AML-15) of the EORTC and GIMEMA leukemia groups. *Haematologica* 89: 950-956, 2004.
- 22 Aplenc R, Alonzo TA, Gerbing RB, Lange BJ, Hurwitz CA, Wells RJ, Bernstein I, Buckley P, Krimmel K, Smith FO, Sievers EL and Arceci RJ; Children's Oncology Group: Safety and efficacy of gemtuzumab ozogamicin in combination with chemotherapy for pediatric acute myeloid leukemia: a report from the Children's Oncology Group. *J Clin Oncol* 26: 2390-2395, 2008.
- 23 Brethon B, Yakouben K, Oudot C, Boutard P, Bruno B, Jérôme C, Nelken B, de Lumley L, Bertrand Y, Dalle JH, Chevret S, Leblanc T and Baruchel A: Efficacy of fractionated gemtuzumab ozogamicin combined with cytarabine in advanced childhood myeloid leukaemia. *Br J Haematol* 143: 541-547, 2008.
- 24 Chevallier P, Delaunay J, Turlure P, Pigneux A, Hunault M, Garand R, Guillaume T, Avet-Loiseau H, Dmytruk N, Girault S, Milpied N, Ifrah N, Mohty M and Harousseau JL: Long-term disease-free survival after gemtuzumab, intermediate-dose cytarabine, and mitoxantrone in patients with CD33(+) primary resistant or relapsed acute myeloid leukemia. *J Clin Oncol* 26: 5192-5197, 2008.
- 25 Chevallier P, Mahe B, Garand R, Talmant P, Harousseau JL and Delaunay J: Combination of chemotherapy and gemtuzumab ozogamicin in adult Philadelphia-positive acute lymphoblastic leukemia patient harboring CD33 expression. *Int J Hematol* 88: 209-211, 2008.
- 26 Clavio M, Vignolo L, Albarello A, Talmant P, Harousseau JL and Delaunay J: Adding low-dose gemtuzumab ozogamicin to fludarabine, Ara-C and idarubicin (MY-FLAI) may improve disease-free and overall survival in elderly patients with non-M3 acute myeloid leukaemia: results of a prospective, pilot, multi-centre trial and comparison with a historical cohort of patients. *Br J Haematol* 138: 186-195, 2007.
- 27 Van PN, Xinh PT, Kano Y, Tokunaga K and Sato Y: Establishment and characterization of a novel Philadelphia-chromosome positive chronic myeloid leukemia cell line, TCC-S, expressing *P210* and *P190 BCR/ABL* transcripts but missing normal *ABL* gene. *Hum Cell* 218: 25-33, 2005.
- 28 Kano Y, Sakamoto S, Kakahara T, Akutsu M, Inoue Y and Miura Y: *In vitro* effects of amsacrine in combination with other anticancer agents. *Leuk Res* 15: 1059-1066, 1991.
- 29 Steel GG and Peckham MJ: Exploitable I mechanisms in combined radiotherapy-chemotherapy: the concept of additivity. *Int J Radiat Oncol Biol Phys* 5: 85-93, 1979.
- 30 Kano Y, Ohnuma T, Okano T and Holland JF: Effects of vincristine in combination with methotrexate and other antitumor agents in human acute lymphoblastic leukemia cells in culture. *Cancer Res* 48: 351-356, 1988.
- 31 Kano Y, Suzuki K, Akutsu M, Inoue Y, Yoshida M, Sakamoto S and Miura Y: Effects of CPT-11 in combination with other anticancer agents in culture. *Int J Cancer* 50: 604-610, 1992.
- 32 Kano Y, Akutsu M, Tsunoda S, Suzuki K and Adachi K: *In vitro* schedule-dependent interaction between paclitaxel and SN-38 (the active metabolite of irinotecan) in human carcinoma cell lines. *Cancer Chemother Pharmacol* 42: 91-98, 1998.
- 33 Dowell JA, Korth-Bradley J, Liu H, King SP and Berger MS: Pharmacokinetics of gemtuzumab ozogamicin, an antibody-targeted chemotherapy agent for the treatment of patients with acute myeloid leukemia in first relapse. *J Clin Pharmacol* 41: 1206-1214, 2001.
- 34 DiJoseph JF, Armellino DC, Boghaert ER, Khandke K, Dougher MM, Sridharan L, Kunz A, Hamann PR, Gorovits B, Udata C, Moran JK, Popplewell AG, Stephens S, Frost P and Damle NK: Antibody-targeted chemotherapy with CMC-544: a CD22-targeted immunoconjugate of calicheamicin for the treatment of B-lymphoid malignancies. *Blood* 103: 1807-1814, 2004.
- 35 DiJoseph JF, Dougher MM, Kalyandrug LB, Armellino DC, Boghaert ER, Hamann PR, Moran JK and Damle NK: Antitumor efficacy of a combination of CMC-544 (inotuzumab ozogamicin), a CD22-targeted cytotoxic immunoconjugate of calicheamicin, and rituximab against non-Hodgkin's B-cell lymphoma. *Clin Cancer Res* 12: 242-249, 2006.
- 36 DiJoseph JF, Dougher MM, Armellino DC, Evans DY and Damle NK: Therapeutic potential of CD22-specific antibody-targeted chemotherapy using inotuzumab ozogamicin (CMC-544) for the treatment of acute lymphoblastic leukemia. *Leukemia* 21: 2240-2245, 2007.

Received June 4, 2009

Revised September 9, 2009

Accepted September 25, 2009

